

1 **Mapping the Immunodominance Landscape of SARS-CoV-2 Spike Protein for**
2 **the Design of Vaccines against COVID-19**

3 Bao-zhong Zhang^{2,\$}, Ye-fan Hu^{1,4,\$}, Lin-lei Chen^{3,\$}, Yi-gang Tong^{5,\$}, Jing-chu Hu²,
4 Jian-piao Cai³, Kwok-Hung Chan³, Ying Dou¹, Jian Deng¹, Hua-rui Gong¹,
5 Chaiyaporn Kuwentrai¹, Wenjun Li², Xiao-lei Wang¹, Hin Chu³, Cai-hui Su¹, Ivan
6 Fan-Ngai Hung⁴, Thomas Chung Cheung Yau^{4,*}, Kelvin Kai-Wang To^{3,*}, Kwok Yung
7 Yuen^{3,*}, Jian-Dong Huang^{1,2,*}

8

9 ¹ School of Biomedical Sciences, Li Ka Shing Faculty of Medicine, University of
10 Hong Kong, 3/F, Laboratory Block, 21 Sassoon Road, Hong Kong, China

11 ² Institute of Synthetic Biology, Shenzhen Institutes of Advanced Technology,
12 Chinese Academy of Sciences, 1068 Xueyuan Avenue, University Town, Nanshan,
13 Shenzhen, 518055, China

14 ³ Department of Microbiology, University of Hong Kong, 19/F T Block, Queen Mary
15 Hospital, 102 Pokfulam Road, Hong Kong, China

16 ⁴ Department of Medicine, University of Hong Kong, 4/F Professional Block, Queen
17 Mary Hospital, 102 Pokfulam Road, Hong Kong, China

18 ⁵ Beijing Advanced Innovation Centre for Soft Matter Science and Engineering
19 (BAIC-SM), College of Life Science and Technology, Beijing University of Chemical
20 Technology

21 ^{\$} Equal contribution.

22 ^{*} Corresponding authors.

23

24 **Abstract**

25 The ongoing coronavirus disease 2019 (COVID-19) pandemic is a serious threat to
26 global public health, and imposes severe burdens on the entire human society. The
27 severe acute respiratory syndrome (SARS) coronavirus-2 (SARS-CoV-2) can cause
28 severe respiratory illness and death. Currently, there are no specific antiviral drugs
29 that can treat COVID-19. Several vaccines against SARS-CoV-2 are being actively
30 developed by research groups around the world. The surface S (spike) protein and the
31 highly expressed internal N (nucleocapsid) protein of SARS-CoV-2 are widely
32 considered as promising candidates for vaccines. In order to guide the design of an
33 effective vaccine, we need experimental data on these potential epitope candidates. In
34 this study, we mapped the immunodominant (ID) sites of S protein using sera samples
35 collected from recently discharged COVID-19 patients. The SARS-CoV-2 S protein-
36 specific antibody levels in the sera of recovered COVID-19 patients were strongly
37 correlated with the neutralising antibody titres. We used epitope mapping to
38 determine the landscape of ID sites of S protein, which identified nine linearized B
39 cell ID sites. Four out of the nine ID sites were found in the receptor-binding domain
40 (RBD). Further analysis showed that these ID sites are potential high-affinity SARS-
41 CoV-2 antibody binding sites. Peptides containing two out of the nine sites were
42 tested as vaccine candidates against SARS-CoV-2 in a mouse model. We detected
43 epitope-specific antibodies and SARS-CoV-2-neutralising activity in the immunised
44 mice. This study for the first time provides human serological data for the design of
45 vaccines against COVID-19.

46

47 **Introduction**

48 The coronavirus disease 2019 (COVID-19), a novel infectious disease caused by
49 severe acute respiratory syndrome coronavirus 2, SARS-CoV-2, first emerged in
50 December 2019 and has since become a worldwide pandemic. COVID-19 infections
51 have so far led to over 2 million cases and more than 0.13 million deaths across more
52 than 200 countries and geographical regions around the world. The World Health
53 Organization has launched a worldwide clinical trial called SOLIDARITY to test
54 antiviral treatment options for the novel coronavirus, but as of April 15, 2020, there
55 are no specific drugs for treating COVID-19¹. Many research teams worldwide are
56 racing to develop vaccines against SARS-CoV-2 to combat this novel coronavirus
57 pandemic.

58 Similar to other coronaviruses, SARS-CoV-2 is an enveloped positive-stranded RNA
59 virus with four major structural proteins: S (spike), E (envelope), M (membrane), and
60 N (nucleocapsid) proteins²⁻⁴. The surface S protein is the key that allows SARS-COV-
61 2 to enter into cells⁵, as it plays a role in binding to the cellular receptor and
62 membrane fusion^{5,6}. The SARS-CoV-2 shares 75.96% homology with the 2003
63 SARS-CoV³, and the structure and functional domains of the SARS-CoV-2 S protein
64 have already been identified⁷. The receptor-binding domain (RBD) within the S1
65 domain binds to angiotensin-converting enzyme 2 (ACE2) to facilitate the entry of
66 SARS-CoV-2 into host cells^{6,7}.

67 As of April 8, 2020, there are at least 115 vaccine candidates in active development
68 worldwide⁸. The SARS-CoV-2 S (spike) glycoprotein is the immunogen that is the
69 focus of the majority of the vaccine research. In the absence of *in vivo* and *in vitro*
70 data, researchers have been using *in silico* data based on the IEDB database or other
71 online epitope prediction algorithms⁹⁻¹⁴. However, the *in silico* data is less likely to be
72 useful for vaccine development, because these bioinformatics tools were not
73 optimised for vaccine design. Furthermore, the antigenic properties of S proteins
74 remain elusive, and therefore experimental immunogenic information is urgently
75 needed.

76 Although a putative epitope that binds to antibodies against SARS-CoV-2 has been
77 reported¹⁵, more epitopes with high affinity need to be identified. Information on
78 these epitopes would be useful, particularly in regard to human immunological bias

79 and immunodominance (ID), which might restrict the immune response.
80 Immunodominance is the phenomenon of immunogenic variation among distinct
81 immunogens or antigenic sites on the same immunogen, which has been demonstrated
82 in both CD8⁺ T cells and B cells¹⁶. This phenomenon has restricted the development
83 of effective vaccines for influenza A and other highly variable viruses¹⁷⁻¹⁹. All the
84 methods used to overcome or manipulate these viral immunity restrictions rely on the
85 landscape of immunodominance. It is therefore crucial to map the immunogenicity
86 landscape of the potential epitopes of the S protein to accelerate the development of
87 vaccines.

88 An ideal vaccine against SARS-CoV-2 should induce highly potent neutralising
89 antibodies but should not induce any disease-enhancing antibodies. Previous studies
90 that used the full-length S protein of SARS-CoV to immunise animals resulted in
91 adverse effect after the animals were challenged with SARS-CoV²⁰. Jiang et al.,
92 identified five linear immunodominant (ID) sites in the S protein that did not induce
93 neutralising antibodies. On the contrary, the RBD was found to contain the major
94 neutralising epitopes in the S protein, but did not have any ID sites²¹.

95 In this study, we aimed to map the landscape of ID sites within the S protein of
96 SARS-CoV-2 and compare these results with those of its counterpart in SARS-CoV.
97 Unlike SARS-CoV, we found the RBD of SARS-CoV-2 had linear ID sites in sera
98 samples collected from recently discharged COVID-19 patients. Subsequent
99 microneutralisation tests demonstrated that mice immunised with peptides containing
100 the ID sites within RBD produced neutralising antibodies. Taken together, the RBD of
101 SARS-CoV-2 has a different ID landscape to its counterpart in SARS-CoV.
102 Furthermore, these data can provide guidance on the design of S protein-based SARS-
103 CoV-2 vaccines that might avoid adverse reactions or disease-enhancing effects.

104

105 **Materials and Methods**

106 **Serum specimens from COVID-19 patients**

107 Serum samples were collected from 39 patients with COVID-19 (22 males and 17
108 females) between Jan 26, 2020, and March 18, 2020. Twenty-six patients who were
109 discharged from hospital provided written informed consent under UW 13-265. The
110 other 13 hospitalized patients were sampled under UW 13-372, and written informed
111 consent was waived. Average sampling time from the onset date was 28.7 days (range,
112 14–44 days). The median age of patients was 59.7 years (range, 26-80 years). All
113 patients were diagnosed with COVID-19 by PCR test, and two patients had a severe
114 illness. The diagnostic criteria for SARS-CoV infection followed the clinical
115 description of COVID-19²². The initial laboratory confirmation was performed on
116 nasopharyngeal or sputum specimens at the Public Health Laboratory Centre of Hong
117 Kong. The discharge criteria were clinically stable and negative nucleic acid test
118 twice consecutively (sampling interval \geq 24 hours). Six healthy donors were also
119 sampled under UW 19-470. This study was approved by the Institutional Review
120 Board of the University of Hong Kong/Hospital Authority Hong Kong West Cluster
121 (UW 13-372, UW 13-265, and UW 19-470).

122 **Animal experiments**

123 The SPF BALB/c mice were supplied by the Laboratory Animal Unit of the
124 University of Hong Kong. All animal experiments were approved by the Committee
125 on the Use of Live Animals in Teaching & Research, the University of Hong Kong
126 (CULATR 5312-20). All mice were immunised by distinct vaccines on Day 0 and
127 Day 14.

128 **Synthesis of peptides**

129 All peptides were manufactured by GL Biochem (Shanghai) Ltd in the form of a dry
130 powder. The peptides were generated using solid phase synthesis methods and the
131 quality of the products was monitored by mass spectrometry. All peptides were
132 dissolved in pH 7.4 PBS buffer or 8 M pH 7.0 urea Na₂HPO₄/NaH₂PO₄ buffer.
133 Peptides conjugated to keyhole limpet haemocyanin (KLH) carrier proteins were also
134 purchased from GL Biochem (Shanghai) Ltd. These peptide-conjugated proteins were
135 dissolved in a pH 7.4 PBS buffer.

136

137 **Antibody detection using ELISA**

138 Epitope-specific antibodies were detected by enzyme-linked immunosorbent assay
139 (ELISA). Briefly, all peptides at a final concentration of 0.5 µg/mL in 50 mM pH 9.6
140 Na₂CO₃/NaHCO₃ buffer were coated on ELISA plates (Nunc, Roskilde, Denmark)
141 and incubated overnight at 4°C. Plates were blocked with TBS-5% (w/v) non-fat milk
142 for 3 h at 37°C and washed four times in 0.05% Tween in TBST. Diluted patient or
143 mice sera were added into the wells and incubated for 1 h at 37°C. Plates were
144 washed six times in TBS-0.05% Tween and incubated with HRP-conjugated goat
145 anti-mouse IgG for 1 h at 37°C. The colour was developed using Trimethyl Borane
146 (TMB) solution (Sigma) and absorbance was measured at 450 nm using an ELISA
147 reader. Samples from non-immunised mice or healthy volunteers were used as the
148 controls. The cut-off lines were based on the mean value plus three times the standard
149 deviation.

150 **Identification of T cell epitopes using ELISpot**

151 The T cell responses were detected by enzyme-linked immunosorbent spot (ELISpot)
152 kits (Dakewe Biotech Co., Ltd) following the manufacturer's protocol. Briefly,
153 splenocytes harvested from sacrificed mice were washed and immediately transferred
154 to anti-IFN-γ antibody pre-coated filter plates. For stimulation, splenocytes were co-
155 incubated with distinct epitopes overnight at 37°C. All samples were assayed with
156 positive controls (Phorbol myristate acetate, PMA and Ionomycin) and cells from a
157 reference donor. All images in different wells were captured using a CTL
158 ImmunoSpot ELISpot Analyzer and processed using the ImmunoCapture software
159 (Cellular Technology Ltd., USA).

160 **Microneutralisation tests**

161 Serial two-fold dilutions of heat-inactivated sera (treated at 56°C for 30 minutes) were
162 prepared from a starting dilution of 1:10. The serum dilutions were mixed with equal
163 volumes of 100 TCID₅₀ of SARS-CoV-2 as indicated. After 1 h of incubation at 37°C,
164 35 µL of the virus-serum mixture was added to Vero-E6 cell monolayer for SARS-
165 CoV-2 infection in 96-well microtitre plates in quadruplicate. After 1 h of adsorption,
166 an additional 150 µL of culture medium was added to each well and incubated for 3
167 days at 37°C in 5% CO₂ in a humidified incubator. A virus back-titration was
168 performed without immune serum to assess the input virus dose. The CPE was read at

169 3 days post infection. The highest serum dilution that completely protected cells from
170 CPE in half the wells was estimated using the Reed-Muench method and was taken as
171 the neutralising antibody titre. Positive and negative control sera were included to
172 validate the assay.

173 **Results**

174 **Immune responses and antiviral effects in serum from COVID-19 patients**

175 All serum samples from COVID-19 patients tested positive for SARS-CoV-2 by
176 ELISA assay using plates coated by SARS-CoV-2 lysates (Figure 1A). The profiles of
177 IgG, and IgM, and IgA against S (spike) and N (nucleocapsid) proteins showed that
178 not all patients had elevated antibody titres compared to healthy donors (Figure 1B-G).
179 Generally, high IgG titres against both S and N proteins were present in the sera,
180 samples, and relatively high IgM and IgA responses were also observed in the
181 majority of patients.

182 Our previous work revealed that the correlations between microneutralisation (MN)
183 activity and anti-NP or anti-RBD IgG titres were stronger than the correlation
184 between MN activity and IgM titre²². To further investigate the correlations between
185 MN activity and anti-NP or anti-RBD IgG, IgM, and IgA titres, we carefully analysed
186 the sera from recovered patients. We found MN activity in the sera of 26 out of 39
187 COVID-19 patients. The MN titres were adjusted following previous criteria: MN
188 titres less than 10 were re-designated a value of 5 and MN titres greater than 320 were
189 re-designated a value of 640²². We identified a very strong correlation between anti-
190 RBD IgG titres and MN activity in recovered patients ($R^2 = 0.8009$). The correlations
191 between anti-RBD IgM/IgA titres and MN activity were weaker than for IgG ($R^2 =$
192 0.5130 and 0.5926 , respectively) (Figure 2E, G, I). However, we found very poor
193 correlations between anti-NP IgG/IgM/IgA titres and MN activity. These correlations
194 dropped dramatically when MN activity titres were greater than 1:160 (Figure 2D, F,
195 H). These results suggest that anti-RBD antibodies play an important role in the
196 antiviral immune response.

197

198 **The landscape of immunodominant sites on the S protein in COVID-19 patients**

199 To identify the immunodominant (ID) sites on the SARS-CoV-2 S protein, we
200 mapped the epitopes in 42 peptides spanning the entire extra-membrane domain (21-
201 926) of the S protein with three gaps (106-160, 365-374, and 687-741). Each peptide
202 was between 20 and 25 residues in length with a five-residue overlap. We measured
203 ID sites in terms of the positive rate and the percentage of convalescent sera from
204 COVID-19 patients having positive reactions to the epitope. Here, we used the mean
205 response plus three times the standard deviation in healthy donors as the cut-off value
206 to define positive reactions. The epitope mapping showed nine linear ID sites on the S
207 protein located at 21-45(IDa), 221-245(IDb), 261-285(IDc), 330-349(IDd), 375-
208 394(IDe), 450-469(IDf), 480-499(IDg), 522-646(IDh), and 902-926(IDi), respectively
209 (Figure 3), with an average positive rate of $\geq 50\%$ among all 39 patients. We found the
210 SARS-CoV-2 RBD contained four ID sites, IDd, IDe, IDf, and IDg, whereas the
211 SARS-CoV RBD has no ID sites. Considering the SARS-CoV-2 S protein shares
212 75.96% identity with the SARS-CoV S protein, we found five out of the nine
213 fragments, IDc (79.17%), IDd (90%), IDe (90%), IDh (79.2%), and IDi (96%) were
214 evolutionarily highly conserved in the SARS-CoV S protein. However, only three of
215 the nine ID sites, IDa (63.64%), IDh (79.05%), and IDi (96%) were highly
216 homologous ($>50\%$) to SARS-CoV S protein ID sites. These results suggest that the
217 conserved regions contribute to the immunogenicity of the S protein, whereas the
218 majority of ID sites (6 out of 9) were less likely to be conserved. Interestingly, some
219 epitopes induced personalized immune responses in specific patients. Patient 33 had
220 an extremely strong immune response to epitope S (21-45) with a 40 times increase
221 compared to the cut-off value, whereas the responses of patients 26 to 31 were not
222 significantly different compared to those of healthy donors. A similar response was
223 also observed for S (281-305), which is less likely to be an ID site. (Figure 3A) These
224 results suggest that some unexpected ID sites of the S protein might lead to highly
225 variable immune responses in patients if immunised with certain viral proteins.

226 **Immunodominant sites can generate antiviral protection in a mouse model**

227 To examine if specific ID sites of the S protein can generate immune responses and
228 antiviral effects, we immunised mice with the RBD and two epitopes (S370-395 and
229 S435-479) of the S protein, which were selected based on the results of B cell epitope
230 prediction, toxicity prediction, and allergenicity prediction (Figure 4A, B). The S370-
231 395 and S435-479 epitopes were validated in our epitope mapping assay in patient
232 sera, which showed positive rates of 51.3% and 74.4%, respectively. The ELISA
233 assay showed that mice immunised with the entire RBD, S370-395, and S435-479
234 generated high levels of specific antibodies (Figure 4C, D, E). In the MN test, mice
235 immunised with S370-395, S435-479 or RBD showed viral neutralising titres of
236 1:26.7, 1:16.7, and 1:33.3, respectively (Figure 4F).

237 The landscape of T cell epitopes in the RBD fragment was profiled by ELISpot assay,
238 which revealed a distinct pattern compared to the B cell responses. In the RBD
239 fragment, three of the T cell epitopes, S405-469, S480-499, and S510-521, induced
240 strong adaptive responses after immunisation. Among the epitopes, S370-395, S450-
241 469 and S480-499 were identified as ID sites in human sera (Figure 4G). The S370-
242 395 and S435-479 epitopes are more likely to be both T cell ID sites and B cell ID
243 sites.

244

245 **Immunodominant sites might reveal potent neutralising sites of S protein**

246 To validate the potential functions of ID sites, we highlighted the ID sites in the
247 SARS-CoV-2 S protein structure model containing glycosylation sites²³ (Figure 5A-
248 C). Among ID sites with positive rates ranging from 50% to 60%, five sites were
249 located on the head region of the S protein and two sites were on the stem of the S
250 protein (Figure 5B). Among ID sites with positive rates over 60%, all five epitopes
251 were located on the head of the S protein (Figure 5C). Although the S protein is a
252 glycoprotein, glycosylation modification had limited effects on immunisation. Two
253 glycosylation sites, N331 and N343, were observed in the RBD region, but these sites
254 had no influence on the immune response. In sera from patients, non-glycosylated
255 peptides were able to induce immune responses (Figure 3A, C and Figure 4G, S330-
256 349).

257 The neutralising titre results (Figure 4F) suggest the ID sites have neutralising
258 activities against SARS-CoV-2, although the ID sites in SARS-CoV were unlikely to
259 be neutralising sites²⁰. To further validate the ID sites, we compared the binding
260 residues of the S protein to reported monoclonal antibodies with the ID sites of
261 RBD^{15,24,25}. Interestingly, some binding residues of SARS-CoV-2-specific
262 neutralising antibodies were highly similar to the ID sites (Figure 5). For CR3022, a
263 monoclonal antibody targeting a highly conserved cryptic epitope¹⁵, 14 out of 28
264 binding residues of SARS-CoV-2 RBD were located in ID sites. For F26G19, a
265 mouse antibody, 11 out of 20 sites were located at ID sites, indicating there was likely
266 a relatively high binding affinity to the RBD fragment²⁵. However, for m396, an
267 antibody with relatively low binding affinity to SARS-CoV-2 RBD, only 5 out of 22
268 binding residues were located at ID sites²⁴. This was also the case for R80, another
269 low binding affinity antibody, which had no matching binding residues²⁴. These
270 results suggest that SARS-CoV-2 ID sites are potent neutralising sites for high-
271 affinity antibodies.

272 **Discussion**

273 In this study, we profiled IgG/IgM/IgA levels against the S protein and N protein in
274 the sera of COVID-19 patients (Figure 1). All convalescent sera from the COVID-19
275 patients contained specific antibodies against recombinant SARS-CoV-2 N protein,
276 but not all sera had specific antibodies for the RBD fragment of the S protein. The
277 relatively high immunogenicity of SARS-CoV-2 N protein during infection showed it
278 has potential as an antigen for developing COVID-19 diagnostics (Figure 1). However,
279 amounts of the different antibodies varied across patients. We found that IgM
280 contributed 5%-34% of N protein-specific antibodies, whereas anti-RBD IgM
281 contributed 10%-49% of RBD-specific antibodies. Patients with acute SARS-CoV-2
282 infection displayed highly diverse immune responses, and this diversity remained
283 until convalescence. These diverse immune responses highlight safety concerns such
284 as secondary infections that need to be considered.

285 We also analysed the correlation between S or N protein-specific antibody levels and
286 SARS-CoV-2 neutralising titres. The Spike RBD-specific antibody level displayed a
287 strong linear correlation with MN titres, but not with the N-specific antibody level
288 (Figure 2). This observation suggests that RBD-specific antibodies in the sera of
289 recovered patients might provide antiviral protection mainly through neutralising
290 activity rather than non-neutralising antibodies against the N protein. This suggests
291 that manipulating the RBD-induced immune responses might be more effective for
292 developing COVID-19 vaccines.

293 This is the first reported mapping of the landscape of the ID sites in the S protein of
294 SARS-CoV-2 using sera from COVID-19 patients (Figure 3). The personalized
295 immune response pattern needs to be further investigated as unexpected and highly
296 variable immune responses in some individuals might lead to adverse events or
297 disease-enhancing responses to certain viral proteins used as vaccines. We further
298 tested if the ID sites in the RBD fragment could be used as potential vaccines in mice.
299 We found that epitopes/protein-specific antibody titres exceeded the
300 microneutralisation titres by several orders of magnitude. Considering the relatively
301 low neutralising antibody levels in the recovered patients in this study and in a
302 previous report²⁶, it is reasonable to expect significant differences between specific
303 antibodies and neutralising antibodies. We found there was equivalent antiviral
304 activity from immunisation with epitopes compared to immunisation with the entire

305 RBD fragment (Figure 4). This provides evidence that epitope-based vaccines could
306 offer comparable protection compared to subunit vaccines, but with the potentially
307 better safety.

308 We also compared binding residues of previously identified SARS-CoV-2
309 neutralising antibodies with ID epitopes. The ID sites in the RBD were found to be
310 potent neutralising sites for SARS-CoV-2 (Figure 5). Previous research suggests that
311 it might be better to overcome the immunodominance of non-neutralising antigenic
312 epitopes for SARS-CoV^{20,27}, influenza virus A¹⁶, dengue fever virus²⁸, and human
313 immunodeficiency virus¹⁹, which can potentially enhance the disease. Indeed a prior
314 study on SARS-CoV implicated ID sites in antibody-dependent enhancement
315 (ADE)^{27,29}. Recent research showed that passive immunisation with early
316 convalescent COVID-19 serum in hamsters resulted in significantly lower viral loads
317 in the respiratory tract without apparent differences in the clinical signs and
318 histopathological changes³⁰. Even so, these results provide limited information on ID.
319 We still do not know how to effectively target immunodominance, and we still need
320 to understand the mechanism underlying this phenomenon.

321 Several candidate vaccines against SARS-CoV-2 including mRNA, inactivated virus,
322 and recombinant adenovirus vaccines have started phase I clinical trials in the US and
323 China⁸. However, there are no reports on the targets of these candidate vaccines, and
324 they might have disease-enhancing effects. Our findings provide evidence for using
325 specific linear antigenic epitopes of S protein instead of the entire S protein for
326 vaccines against SARS-CoV-2 with better safety.

327

328

329 **Acknowledgements**

330 We would like to thank the technicians in the laboratories of JD Huang and KY Yuen
331 for their help in running the project. This work was supported by Health and Medical
332 Research Fund (HKM-15-M09), the Shenzhen Peacock Team Project
333 (KQTD2015033117210153), Shenzhen Science and Technology Innovation
334 Committee Basic Science Research Grant (JCYJ20170413154523577) and China
335 Postdoctoral Science Foundation (2019M663167).

336 **Author Contributions**

337 BZ Zhang, YF Hu, LL Chen, YG Tong, TCC Yau, KKW To, KY Yuen, and JD
338 Huang designed the study. IFN Hung recruited all the patients. BZ Zhang, YF Hu, KH
339 Chan, and LL Chen performed the experiments. JC Hu, JP Cai, Y Dou, J Deng, HR
340 Gong, C Kuwentrai, WJ Li, XL Wang, H Chu, and CH Su participated in the study.
341 BZ Zhang, YF Hu, LL Chen, YG Tong, TCC Yau, KKW To, KY Yuen, and JD
342 Huang analysed the data. BZ Zhang, YF Hu, and JD Huang wrote the manuscript.

343 **Competing Interests**

344 The authors declare that they have no competing interests.

345 **Data and Materials Availability**

346 All data used to draw the conclusions in the paper are presented in the paper and/or
347 the supplementary materials.

348

349 **References**

- 350 1. Kupferschmidt K & J, C. WHO launches global megatrial of the four most
351 promising coronavirus treatments. *Science* (2020).
- 352 2. Wu, F., *et al.* A new coronavirus associated with human respiratory disease in
353 China. *Nature* **579**, 265-269 (2020).
- 354 3. Lu, R., *et al.* Genomic characterisation and epidemiology of 2019 novel
355 coronavirus: implications for virus origins and receptor binding. *The Lancet* **395**,
356 565-574 (2020).
- 357 4. Zhou, P., *et al.* A pneumonia outbreak associated with a new coronavirus of
358 probable bat origin. *Nature*, 1-4 (2020).
- 359 5. Hoffmann, M., *et al.* SARS-CoV-2 cell entry depends on ACE2 and TMPRSS2
360 and is blocked by a clinically proven protease inhibitor. *Cell* (2020).
- 361 6. Yan, R., *et al.* Structural basis for the recognition of SARS-CoV-2 by full-length
362 human ACE2. *Science* **367**, 1444-1448 (2020).
- 363 7. Wrapp, D., *et al.* Cryo-EM structure of the 2019-nCoV spike in the prefusion
364 conformation. *Science* **367**, 1260-1263 (2020).
- 365 8. Le, T.T., *et al.* The COVID-19 vaccine development landscape. *Nature Reviews*
366 *Drug Discovery* (2020).
- 367 9. Grifoni, A., *et al.* A Sequence Homology and Bioinformatic Approach Can Predict
368 Candidate Targets for Immune Responses to SARS-CoV-2. *Cell host & microbe*
369 (2020).
- 370 10. Ahmed, S.F., Quadeer, A.A. & McKay, M.R. Preliminary identification of potential
371 vaccine targets for the COVID-19 coronavirus (SARS-CoV-2) based on SARS-
372 CoV immunological studies. *Viruses* **12**, 254 (2020).
- 373 11. Bhattacharya, M., *et al.* Development of epitope-based peptide vaccine against
374 novel coronavirus 2019 (SARS-COV-2): Immunoinformatics approach. *Journal of*
375 *Medical Virology* (2020).
- 376 12. Zheng, M. & Song, L. Novel antibody epitopes dominate the antigenicity of
377 spike glycoprotein in SARS-CoV-2 compared to SARS-CoV. *Cellular &*
378 *molecular immunology*, 1-3 (2020).
- 379 13. Fast, E. & Chen, B. Potential T-cell and B-cell Epitopes of 2019-nCoV. *bioRxiv*
380 (2020).
- 381 14. Lucchese, G. Epitopes for a 2019-nCoV vaccine. *Cellular & Molecular*
382 *Immunology*, 1-2 (2020).
- 383 15. Yuan, M., *et al.* A highly conserved cryptic epitope in the receptor-binding
384 domains of SARS-CoV-2 and SARS-CoV. *Science* (2020).
- 385 16. Angeletti, D. & Yewdell, J.W. Understanding and manipulating viral immunity:
386 antibody immunodominance enters center stage. *Trends in immunology* **39**,
387 549-561 (2018).
- 388 17. Dale, G.A., Shartouny, J.R. & Jacob, J. Quantifying the shifting landscape of B cell
389 immunodominance. *Nature immunology* **18**, 367-368 (2017).
- 390 18. Angeletti, D., *et al.* Defining B cell immunodominance to viruses. *Nature*
391 *immunology* **18**, 456 (2017).
- 392 19. Cirelli, K.M., *et al.* Slow delivery immunization enhances HIV neutralizing
393 antibody and germinal center responses via modulation of immunodominance.
394 *Cell* **177**, 1153-1171. e1128 (2019).

- 395 20. Jiang, S., He, Y. & Liu, S. SARS vaccine development. *Emerging infectious*
396 *diseases* **11**, 1016 (2005).
- 397 21. He, Y., *et al.* Identification of immunodominant sites on the spike protein of
398 severe acute respiratory syndrome (SARS) coronavirus: implication for
399 developing SARS diagnostics and vaccines. *The Journal of Immunology* **173**,
400 4050-4057 (2004).
- 401 22. To, K.K.-W., *et al.* Temporal profiles of viral load in posterior oropharyngeal
402 saliva samples and serum antibody responses during infection by SARS-CoV-2:
403 an observational cohort study. *The Lancet Infectious Diseases* (2020).
- 404 23. Walls, A.C., *et al.* Structure, function, and antigenicity of the SARS-CoV-2 spike
405 glycoprotein. *Cell* (2020).
- 406 24. Tian, X., *et al.* Potent binding of 2019 novel coronavirus spike protein by a SARS
407 coronavirus-specific human monoclonal antibody. *Emerging microbes &*
408 *infections* **9**, 382-385 (2020).
- 409 25. Park, T., *et al.* Spike protein binding prediction with neutralizing antibodies of
410 SARS-CoV-2. *bioRxiv* (2020).
- 411 26. Wu, F., *et al.* Neutralizing antibody responses to SARS-CoV-2 in a COVID-19
412 recovered patient cohort and their implications. (2020).
- 413 27. Wang, Q., *et al.* Immunodominant SARS coronavirus epitopes in humans elicited
414 both enhancing and neutralizing effects on infection in non-human primates.
415 *ACS infectious diseases* **2**, 361-376 (2016).
- 416 28. Hughes, H.R., Crill, W.D. & Chang, G.-J.J. Manipulation of immunodominant
417 dengue virus E protein epitopes reduces potential antibody-dependent
418 enhancement. *Virology journal* **9**, 115 (2012).
- 419 29. Liu, L., *et al.* Anti-spike IgG causes severe acute lung injury by skewing
420 macrophage responses during acute SARS-CoV infection. *JCI insight* **4**(2019).
- 421 30. Chan, J.F.-W., *et al.* Simulation of the clinical and pathological manifestations of
422 Coronavirus Disease 2019 (COVID-19) in golden Syrian hamster model:
423 implications for disease pathogenesis and transmissibility. *Clinical Infectious*
424 *Diseases* (2020).

425

426

427 **Figure Legends and Table**

428 **Figure 1. Detection of antibodies specific for SARS-CoV-2 proteins in early**
429 **convalescent sera from COVID-19 patients by ELISA.** (A) Total proteins from
430 SARS-CoV-2 lysates were used as the coated antigen. (B-D) The recombinant N
431 protein was used as the coated antigen. (E-G) The recombinant SP_RBD protein was
432 used as the coated antigen. (H-I) Antibody isotyping of N and SP_RBD binding
433 antibodies in early convalescent sera from COVID-19 patients. Sera from 39 COVID-
434 19 patients, and 6 healthy blood donors were tested at a dilution of 1:100. The dashed
435 lines represent cut-off values (the mean absorbance at 450 nm of sera from healthy
436 blood donors plus three times the standard deviation).

437

438 **Figure 2. Correlations between S or N protein-specific antibody titres and**
439 **microneutralisation antibody titres.** (A-C) N protein or RBD fragment of S protein-
440 specific IgG levels and microneutralisation (MN) assay results of recovered patients'
441 antibody titres. (D-E) Correlation between N protein or RBD fragment of S protein-
442 specific IgG levels and microneutralisation antibody titres. (F-G) Correlation between
443 N protein or RBD fragment of S protein-specific IgM levels and microneutralisation
444 antibody titres. (H-I) Correlation between N protein or RBD fragment of S protein-
445 specific IgA levels and microneutralisation antibody titres.

446

447 **Figure 3. Epitope landscape of SARS-CoV-2 S proteins in convalescent sera from**
448 **COVID-19 patients by ELISA.** (A) The landscape of adjusted epitope-specific
449 antibody levels in each patient. The ELISA results of absorbance at 450 nm were
450 normalized to the aforementioned cut-off values. (B) Schematic representation of
451 SARS-CoV-2 S protein and identified immunodominant sites. Here, only epitopes
452 with positive rates greater than 50% are immunodominant. (C) Positive rates of
453 distinct epitopes of SARS-CoV-2 S protein.

454

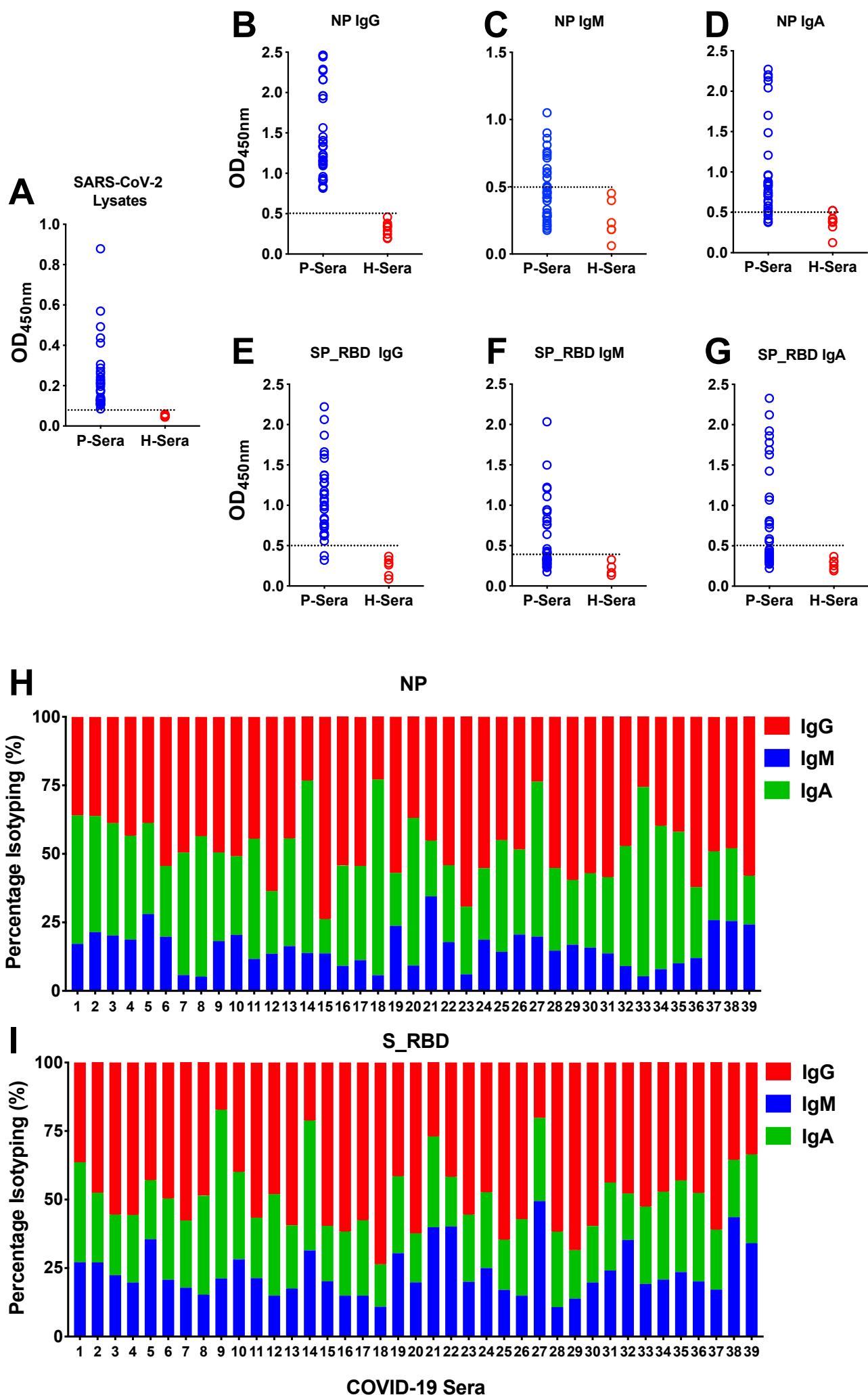
455 **Figure 4. B Cell and T Cell responses to distinct epitopes in SARS-CoV-2**
456 **immunised mice.** (A-B) Schematic representation of the mouse immunisation
457 schedule. Balb/C mice (n = 5 per group) were immunised subcutaneously (s.c) with
458 25 µg of rRBD and KLH-conjugated peptides S370-395 and S435-479 mixed with

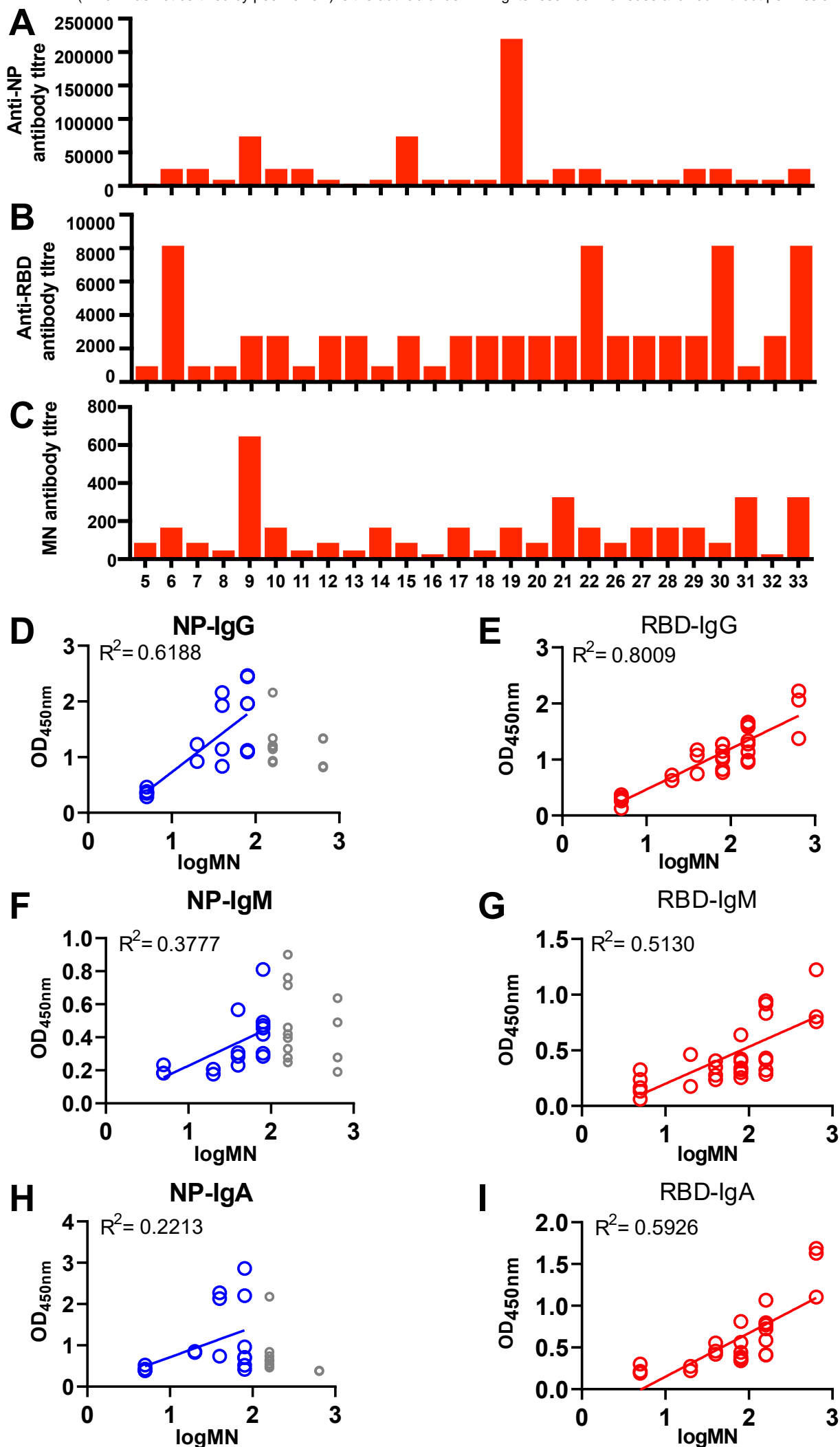
459 aluminium hydroxide gel (AHG). (C-E) rRBD-specific antibody responses in
460 immunised mice. rRBD-specific IgG antibody responses in mouse sera collected at 7
461 days after the second vaccination. (F) Virus microneutralisation antibody titres were
462 measured against SARS-CoV-2 in classical BSL3. (G) Number of IFN- γ -secreting
463 splenocytes in response to stimulation with the 12 RBD peptide pools of 20-mer
464 peptides. SFU: spot-forming units

465

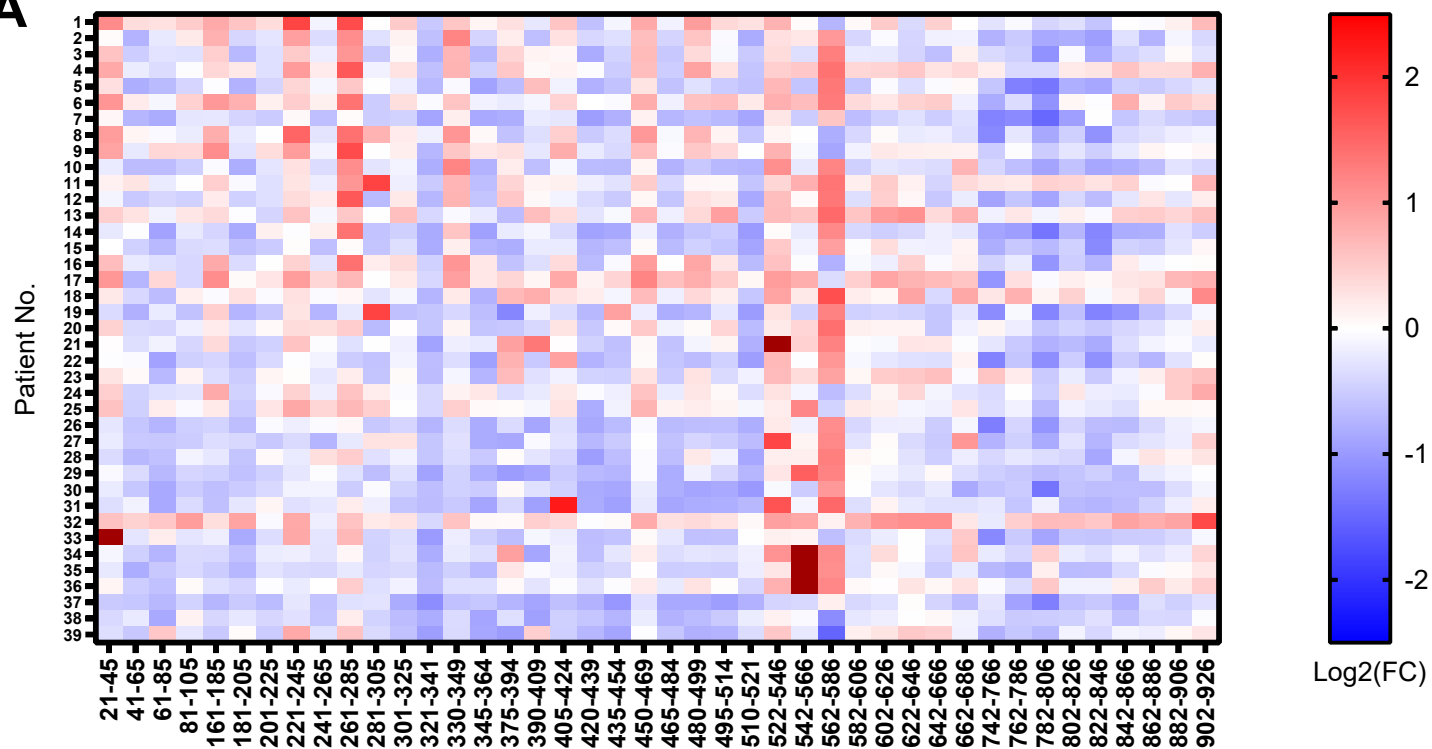
466 **Figure 5. Structural representation of immunodominant and potential**
467 **neutralising sites in SARS-CoV-2 RBD.** (A) Top view and side view of the S (spike)
468 protein in trimer form with labelled RBD region and glycosylation sites. (B) Top view
469 and side view of the S (spike) protein with immunodominant sites with positive rates
470 ranging from 50% to 60%. (C) Top view and side view of the S (spike) protein with
471 immunodominant sites with positive rates greater than 60%. (D) Amino acid sequence
472 alignment of SARS-CoV-2 and SARS-CoV RBD sequences. Related neutralising
473 antibody binding sites, ACE2 binding sites, prominent alterations, and
474 immunodominant sites of SARS-CoV-2 and SARS-CoV are shown.

475

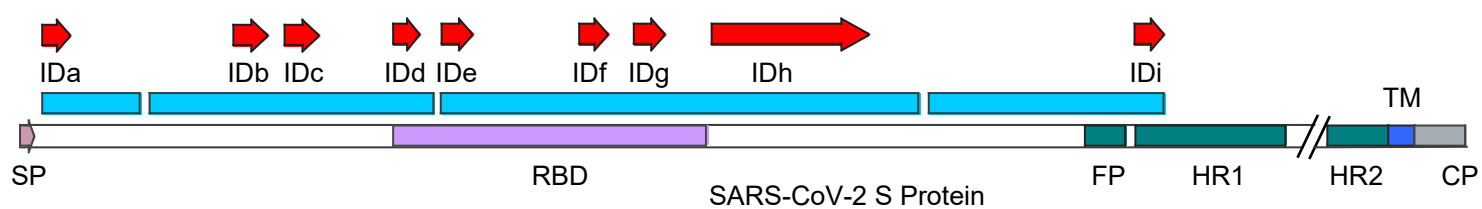




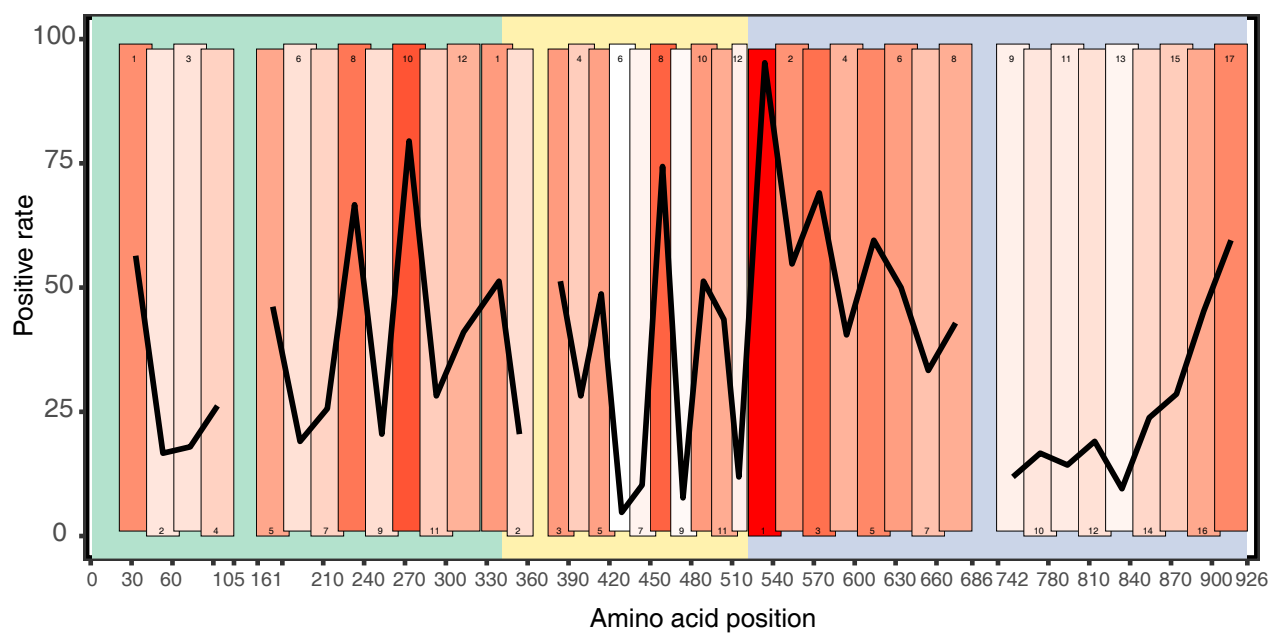
A



B



C



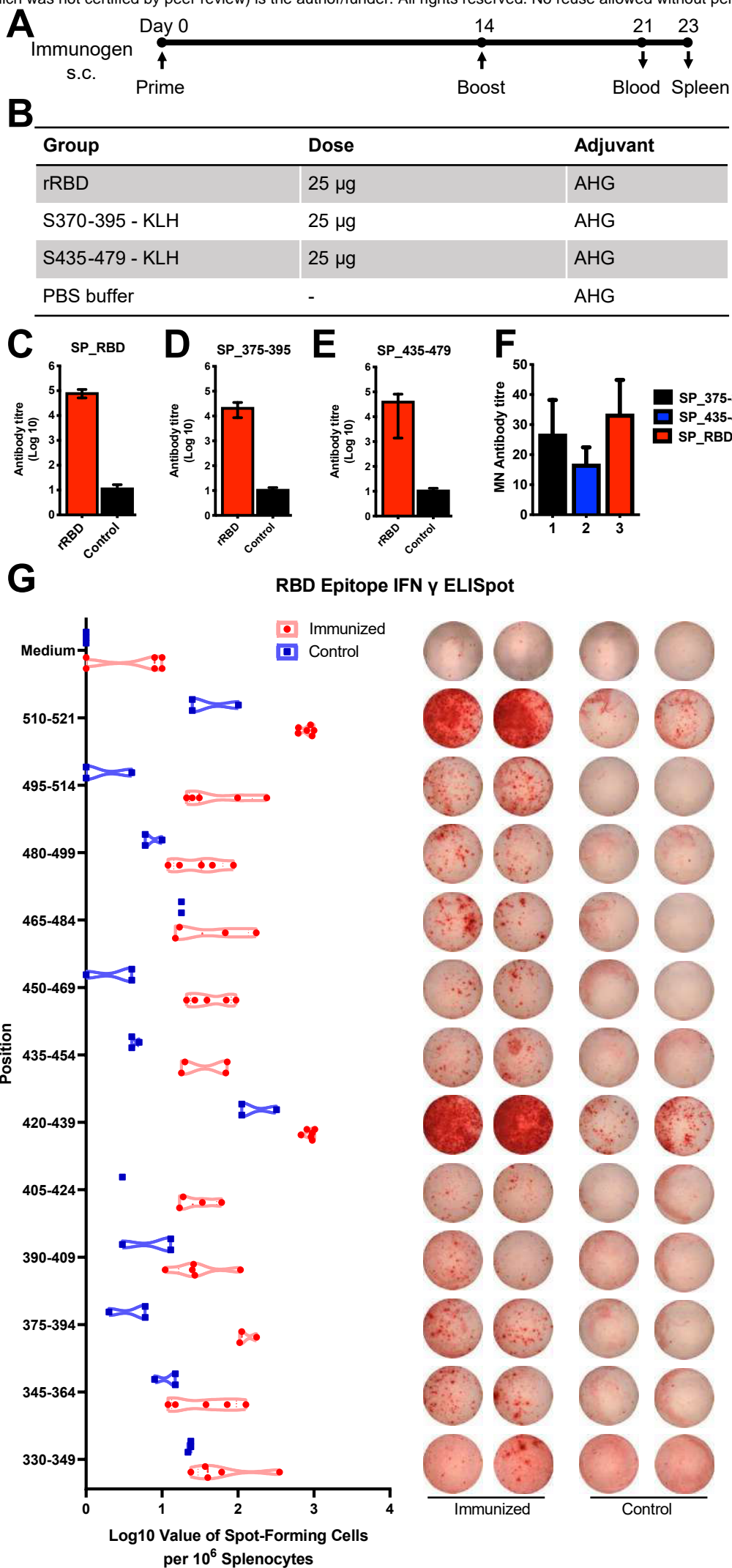
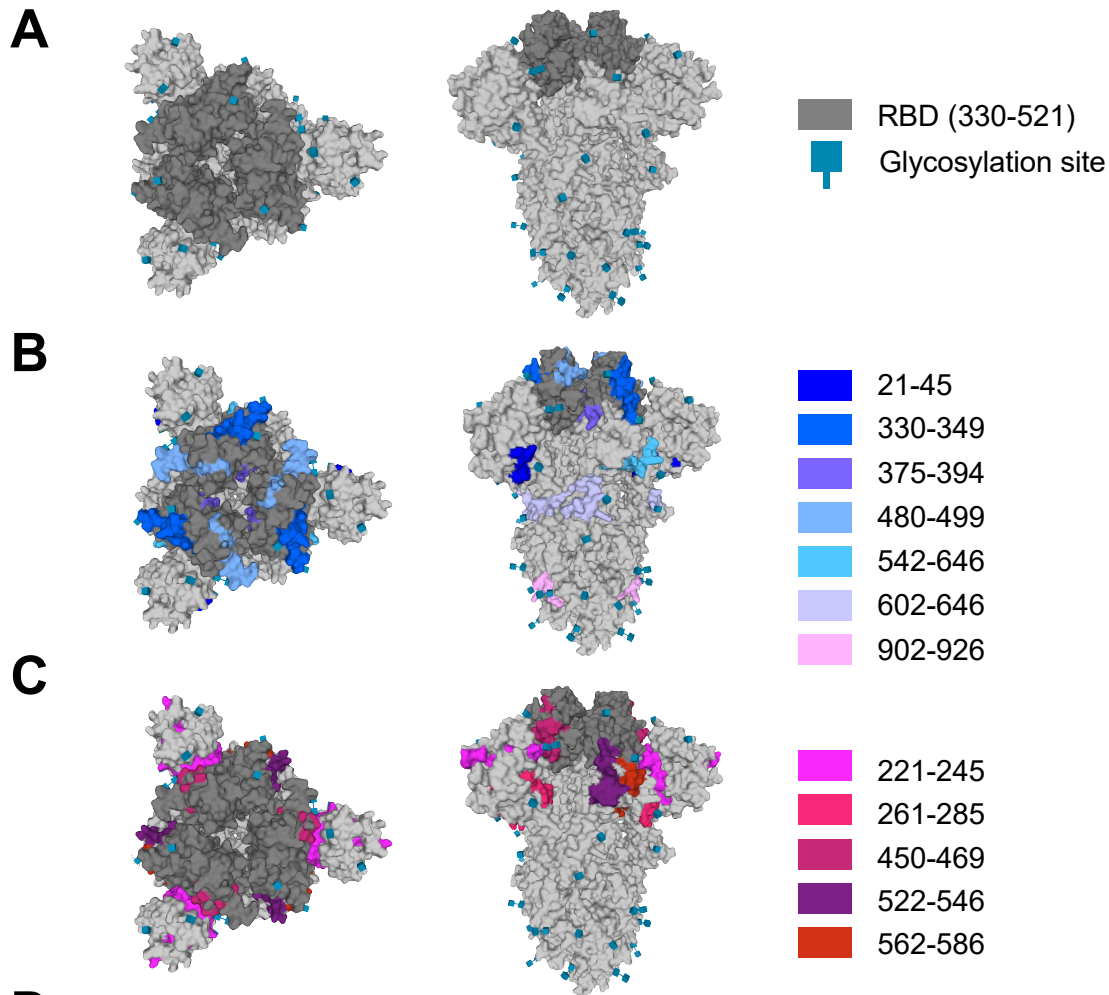


Figure 5



D

SARS-CoV-2 295 PLSETKCTLKSFTEVEKGIYQTSNFRVQPOTESIVREFNITNLCPFGEVFNATRFASVYAWN 354

PL E KC KSF ++KGIYQTSNFRV P +VREFNITNLCPFGEVFNAT F SVYAW

SARS-CoV 282 PLAE**ELKCSVK**SFEIDKGIYQTSNFRVVP**SGD**VVREFNITNLCPFGEVFNATK**FP**SVYAW 341

. * * * * * * * *

SARS-CoV-2 355 RKRISNCVADYSVL**YN**SA**SFSTFKCYGVS**PTK**LN**DL**CF**TVYADSFVIRGDEV**RQ**IAPG**Q** 414

RK ISNCVADYSVL**YN**S FSTFKCYGVS T**KL**N**D**L**CF** NVYADSFV+ GD+VR**Q**IAPG**Q**

SARS-CoV 342 RKRISNCVADYSVL**YN**ST**FF**S**T**FKCYGVSAT**KL**N**D**L**CF**SNVYADSFV**VK**GD**D**VR**Q**IAPG**Q** 401

. * * * * * * * *

▽ # # # ▽ ▽ #

SARS-CoV-2 415 T**G**KIADY**N**Y**K**LP**D**D**F**T**G**CVIA**W**NS**N**LD**S**K**V**GG**N**Y**NY**LY**R**L**F**R**K**S**N**L**K**P**F**E**R**D**I**S**TE**I**Y**Q 474

T**G** IADY**N**Y**K**LP**D**D**F** G**C**V **A**W**N** **N** **D** G**N**Y**N**Y **Y**R **R** **L** P**F**E**R**D**I**S **+**

SARS-CoV 402 T**G**VIADY**N**Y**K**LP**D**D**F**M**G**CVL**A**W**N**TR**N**I**D**A**T**ST**G**N**Y**N**Y**K**Y**R**L**R**H**G**K**L**R**P**F**E**R**D**I**S**N**V**P**F**S** 461

↑ # # # # # # # # ↑↑

. * * * * * * *

▽▽ ▽ ▽ ▽ ▽ ▽ # # # # # # # # # # # # # #

SARS-CoV-2 475 A**G**S**T**P**C****N**G**V**E**G**F**N**C**Y**F**F**L**P**L**Q**S**Y**G**F**O**H**T**N**G**V**G**Y**Q**P**Y**R**V**V**L**S**F**E**L**L**H**A**P**A**T**V**C**G**P**K**R**S**T**N**L**V** 534

PC **N**C**Y** **P**L **Y**G**F** **T** **G**+**G**Y**Q**P**Y**R**V**V**L**S**F**E**L**L **A**P**A**T**V**C**G**P**K** **S**T**+**L**+**

SARS-CoV 462 **P**D**G**K**P**C**T**P**-**P**A**L**N**C**Y**W**L**N**D**Y**G**F**Y**T**T**T**G**I**G**Y**Q**P**Y**R**V**V**L**S**F**E**L**L**N**A**P**A**T**V**C**G**P**K**L**S**T**D**L**I 520

↑ * * * * * * * *

#

△△△ △△△ △△△ △△△ △△△ △△△ △△△ △△△

_ CR3022 * m396 . 80R # F26G19 △ACE2

□ Glycosylation site † Prominent Alteration SARS-CoV-2 ID SARS-CoV ID